Front. Environ. Sci. Eng., 2016, 10(4): 15
DOI 10.1007/s11783-016-0860-z

RESEARCH ARTICLE

An electrochemical process that uses an Fe^0/TiO_2 cathode to degrade typical dyes and antibiotics and a bio-anode that produces electricity

Chaojie Jiang[1], Lifen Liu (✉)[1], John C. Crittenden[2]

1 Key Laboratory of Industrial Ecology and Environmental Engineering (Ministry of Education), School of Environmental Science and Technology, Dalian University of Technology, Dalian 116024, China
2 School of Civil and Environmental Engineering, Georgia Institute of Technology, Atlanta, GA 30332, USA

HIGHLIGHTS

- A bio-electrochemical fuel cell reactor with cathodic Fe^0/TiO_2 generates electricity.
- It destroys recalcitrant pollutants in cathode chamber without photocatalysis.
- Fe^0/TiO_2 generates reactive oxygenated species in the dark or under photocatalysis.
- Cathodic produced ROS (hydroxy radical/superoxide radical) can degrade tetracycline or dyes.
- Electricity generation is enhanced by semiconductor catalyzed cathodic degradation of pollutants.

GRAPHIC ABSTRACT

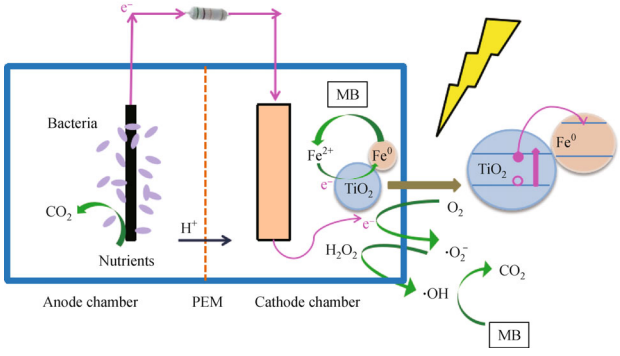

ARTICLE INFO

Article history:
Received 14 February 2016
Received in revised from 7 May 2016
Accepted 12 June 2016

Keywords:
Bio-anode
Photocatalytic cathode
Fe^0/TiO_2
ESR
Dye and antibiotics
Advanced oxidation

ABSTRACT

In this study, a new water treatment system that couples (photo-) electrochemical catalysis (PEC or EC) in a microbial fuel cell (MFC) was configured using a stainless-steel (SS) cathode coated with Fe^0/TiO_2. We examined the destruction of methylene blue (MB) and tetracycline. Fe^0/TiO_2 was prepared using a chemical reduction-deposition method and coated onto an SS wire mesh (500 mesh) using a sol technique. The anode generates electricity using microbes (bio-anode). Connected via wire and ohmic resistance, the system requires a short reaction time and operates at a low cost by effectively removing 94% MB (initial concentration 20 $mg \cdot L^{-1}$) and 83% TOC/TOC_0 under visible light illumination (50 W; 1.99 $mW \cdot cm^{-2}$ for 120 min, MFC-PEC). The removal was similar even without light irradiation (MFC-EC). The E_{Eo} of the MFC-PEC system was approximately 0.675 $kWh \cdot m^{-3} \cdot order^{-1}$, whereas that of the MFC-EC system was zero. The system was able to remove 70% COD in tetracycline solution (initial tetracycline concentration 100 $mg \cdot L^{-1}$) after 120 min of visible light illumination; without light, the removal was 15% lower. The destruction of MB and tetracycline in both traditional photocatalysis and photoelectrocatalysis systems was notably low. The electron spin-resonance spectroscopy (ESR) study demonstrated that ·OH was formed under visible light, and $\cdot O_2^-$ was formed without light. The bio-electricity-activated O_2 and ROS (reactive oxidizing species) generation by Fe^0/TiO_2 effectively degraded the pollutants. This cathodic degradation improved the electricity generation by accepting and consuming more electrons from the bio-anode.

1 Introduction

With the rapid increase in population and industrial development, many organic pollutants are discharged

✉ Corresponding author
E-mail: lifenliu@dlut.edu.cn

into the water and cause severe environmental contamination [1]. Efficient treatment of wastewater is notably important to control global water contamination. For persistent chemical pollutants, their treatment can be very costly and require more energy [2] and their presence in water threatens human health and social development [3].

The efficacy of water treatment is measured in terms of both efficiency and energy consumption (EC). Processes such as aerobic membrane bioreactors, ozonation and advanced oxidation are often energy- and capital-intensive [2]. Therefore, developing low-energy and low-cost effective treatment technologies [3] is a high priority.

Environmentally friendly microbial fuel cell (MFC) technology has recently gathered much attention [4]. It is a promising technology that both produces electricity and treats wastewater using microorganisms to oxidize organics [5–9]. This technology contributes to solving two major problems that water purveyors face: water availability and energy use [10,11]. In an MFC, electrons from the microbial metabolism are conducted from the anode and transferred to the cathode through an external electric circuit, where they combine with electron acceptors and protons in the cathodic compartment [11,12]. However, its unique advantages are limited due to certain shortcomings, such as the low power density output, high internal resistance [4] and poor efficiency in removing refractory pollutants. Until recently, MFC-based wastewater treatment processes have been developed to enhance the pollutant removal efficiencies and bio-electricity generation [13]. Some unique options that may be coupled to an MFC include (1) pollutant degradation by electro-catalysis (EC) on a cathode using E-Fenton catalysts and (2) integration with photo-electro-catalysis (PEC) or a photocatalytic fuel cell (PFC), which may enhance the treatment efficiency and generate more electricity. To date, few studies on the coupling of a PEC system and an MFC have been performed; this study will focus on this topic.

PEC is considered more effective than photocatalysis (PC), although both systems are attractive treatment and solar energy conversion technologies [14–16]. The valence band holes and the ROS, which is formed by PC or PEC, are powerful oxidants to degrade refractory organic compounds [17]. PEC, which is assisted by an external electric circuit, can more effectively oxidize pollutants [16] than PC. Studies about PC anodes are common, but those about PC cathodes and their applications are not.

It is critical to design a high-performance catalyst to enhance the use of solar energy and improve the efficiency of water treatment [2]. Although many catalysts with diverse photocatalytic performance have been studied, TiO_2 remains widely used because of its high photocatalytic activity, low cost and stability [18–20] for destroying various pollutants, such as organic chlorine-containing pesticides, PCBs, and organic dyes [19,21,22]. Recently, Wang et al. [23] investigated the excited electronic state structure of the typical rutile TiO_2 (110) surface using two-photon photoemission spectroscopy (2PPE) and density functional theory (DFT) calculations. They identified an excited resonant state centered at 2.5 ± 0.2 eV above the Fermi level, which is associated with Ti^{3+} species in reduced TiO_2. This result points to an interesting application of TiO_2 in electro-catalysis as a cathode.

However, TiO_2 has a large band gap and can only absorb UV light; it also has a low quantum yield, which limits its application. Intense efforts have been made to improve its visible light usage efficiency [24], such as doping with metal ions, nonmetal ions and other semiconductors. Many studies focused on its doping with Fe^{3+} have achieved satisfactory results. However, only a few studies refer to its doping with Fe^0. Nano-scale zero-valent iron has been demonstrated to effectively reduce organic compounds in aqueous solutions because of its great reducing ability, low cost and environmental safety [25]. In related studies, which included an iron plate anode with microbes, a maximum power density of 4343 $mW \cdot m^{-2}$ was obtained when the ionic strength of the solution was 0.56 M [26]. Thus, more research is warranted in this field.

In this study, we developed a new system called MFC-PEC, which couples photo-PEC with microbial fuel cells (MFCs) to destroy typical pollutants: methylene blue (MB) and tetracycline. The other new component of this study is the development of a cathodic Fe^0/TiO_2 catalyst and an evaluation of its performance when coupled to a bio-anode. The cathode catalyst was prepared using a chemical reduction-deposition method and coated onto the surface of a stainless-steel wire mesh using a silica sol gel method. The microbes at the anode produce electricity, which helps power the destruction of organics at the cathode. The new MFC-PEC system is more capable of destroying the two typical organics than pure PC or PEC systems while maintaining a higher cell voltage. Furthermore, these results were surprisingly achieved within a shorter reaction time and at a lower cost.

2 Materials and methods

2.1 Preparation of Fe^0/TiO_2

Fe^0/TiO_2 was synthesized by chemical reduction using $NaBH_4$ [27]. Figure 1 shows the flow chart of preparing the catalytic cathode electrode, which can be enumerated as follows. (1) $FeSO_4 \cdot 7H_2O$ (0.050 g) was added into a beaker that contained TiO_2 powder (1.000 g). (2) Nanopure water was added until the solution volume was 50 mL. (3) The mixture was dispersed for 20 min using ultrasonic technology. (4) The solution was bubbled with nitrogen for 30 min. (5) $NaBH_4$ (0.0136 g) was added into the beaker and bubbled using nitrogen for another 30 min. (6) The mixture was centrifuged and subsequently

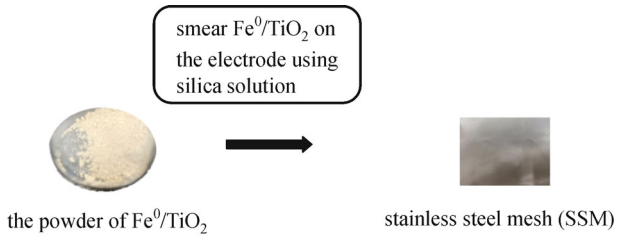

Fig. 1 Flow chart of the catalytic cathode preparation

washed with deionized water and alcohol twice. (7) Finally, it was dried in a vacuum oven at 60°C for at least 4 h.

2.2 Preparation of a silica sol solution as the binder

The silica sol binder was prepared as follows. (1) Alcohol and tetraethyl orthosilicate were placed into a beaker. (2) Next, 36% HCl was added to the mixture. (3) Nanopure water was added in a drop-wise manner (the volume ratio of these four types of liquids was 40: 18: 9.8: 36). (4) Finally, after 30 min of stirring, the gel solution was formed, transferred into a plastic bottle, and stored in a cool place.

2.3 Preparation of the electrode

The base material for the cathode electrode was a stainless-steel wire mesh, and its surface was brush-coated with Fe^0/TiO_2 using the silica sol solution. Then, the electrode was dried in a vacuum oven at 60°C for approximately 15 min.

2.4 The PC, PEC and MFC-PEC/EC systems

The visible light source used in this study was a halogen lamp (50 W; 1.99 $mW \cdot cm^{-2}$). A germicidal UV lamp (0.297 $mW \cdot cm^{-2}$; 254 nm) was used for comparison.

The experiments to destroy MB or tetracycline in the PC and PEC systems were performed using a 150 mL beaker; the initial concentrations of the MB and tetracycline solutions were 20 $mg \cdot L^{-1}$ (100 mL) and 100 $mg \cdot L^{-1}$ (100 mL), respectively. The distance between the visible light source and the liquid level was approximately 5 cm.

Figure 2 displays the design of our new MFC-PEC/EC system. Fe^0/TiO_2 was placed into the cathode chamber, and granular activated carbon was put into the anode chamber. The two chambers were connected via a wire with a resistor. The cathode and anode chambers were connected with a piece of proton exchange membrane (PEM). In this part, the concentrations of the MB and tetracycline solutions to be degraded were 20 $mg \cdot L^{-1}$ (200 mL) and 100 $mg \cdot L^{-1}$ (200 mL), respectively. The visible light source was placed beside the wall of the cathode chamber, which was made of quartz. The distance between the visible light source and the quartz was approximately 5 cm.

Fig. 2 Design of the MFC-PEC system

Air was aerated into the cathode chamber at 0.1 $m^3 \cdot h^{-1}$. The illuminated area was approximately 45 cm^2.

2.5 The calculation of electrical energy efficiency

Electrical energy per order (E_{Eo}) is defined as the required number of kilowatt hours of electrical energy to reduce the concentration of a pollutant by 1 order of magnitude (90%) in a unit volume of contaminated water [28–31]. E_{Eo} (kWh $\cdot m^{-3} \cdot order^{-1}$) is calculated as follows:

$$E_{Eo} = \frac{P \times t \times 1000}{V \times 60 \times \log(C_0/C)}. \quad (1)$$

In this equation, P is the input power (kW) to the system, t is the irradiation time (min), V is the volume of water (L) in the reactor, and C_0 and C are the initial and final pollutant concentrations, respectively.

2.6 Analytical methods

Fe^0/TiO_2 was characterized using scanning electron microscope (SEM, QUANTA 450, FEI, USA) and UV-vis (LAMBDA 950, PerkinElmer, USA). The concentration and TOC of MB were measured using an ultraviolet and visible spectrophotometer (UV762, INSEA, China) and a TOC/TN_b analyzer (multi N/C 2100S, analytikiena, Germany), respectively. The COD of the tetracycline solution was measured using a COD rapid measurement instrument (COD-571, INSEA, China). The formed radicals were trapped using DPMO and characterized using ESR (A200, Bruker, Germany) to explore the mechanism. To measure the cell voltage of the MFC-PEC/EC system, a data acquisition card (MPS-010602, China) was used to measure the voltage over the ohmic resistance (500 Ω).

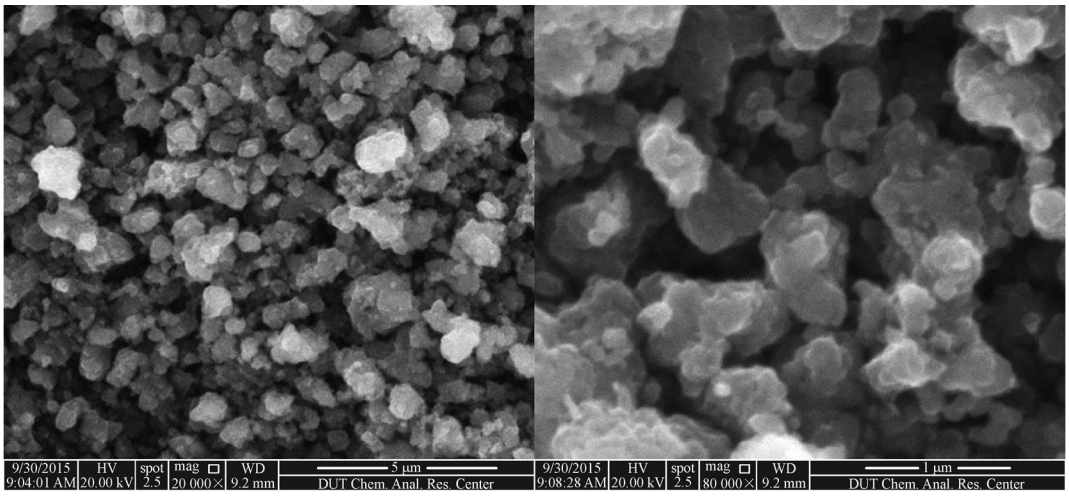

Fig. 3 SEM images of nanoscale Fe^0/TiO_2 composites

3 Results and discussion

3.1 Characterization of the Fe^0/TiO_2 cathode

The SEM images of Fe^0/TiO_2 are shown in Fig. 3. The Fe^0/TiO_2 spherical aggregates were approximately 300 nm in diameter, although some were smaller and approximately 80 nm in diameter.

The UV-vis absorption spectra of TiO_2 and nanoscale Fe^0/TiO_2 composites are shown in Fig. 4. The Fe^0 addition caused significant absorption in the visible region. The Fe^0-doped TiO_2 had absorption in both the UV and visible light regions. Furthermore, the redshift, which is the shifting of absorption edges to a longer wavelength, signifies a decrease in the band gap [32]. A narrower band gap and increased light absorption can increase the yield of photogenerated electron-hole pairs, which is beneficial for the pollutant degradation under visible light [27].

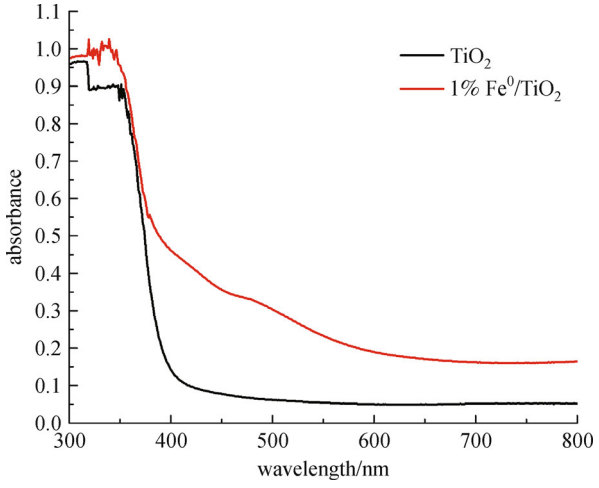

Fig. 4 UV-vis absorption spectra of TiO_2 and nanoscale Fe^0/TiO_2 composites

3.2 Degradation of pollutants

Figures 5(a) and 5(b) show the destruction of MB in the cathodic chamber under four different circumstances: (1) only Fe^0/TiO_2 and photocatalysis (PC); (2) Fe^0/TiO_2 (anode) and Pt (cathode) connected with light (PEC); (3) the bio-anode and Fe^0/TiO_2 cathode connected with light irradiation (MFC-PEC); and (4) the bio-anode and Fe^0/TiO_2 (cathode) connected without light irradiation (MFC-EC).

The MB concentration decreased by 94.84% after a reaction time of 120 min in our new MFC-PEC system (Fig. 5(a)), and the result in the MFC-EC system was nearly 90.98%. There is a striking contrast because the decrease in the MB concentration in the PC and PEC systems was much lower than the aforementioned result for the new system. Furthermore, the reduction in MB for the PC system was only approximately 30% after 120 min. The adsorption in the MFC-PEC system was approximately 9% of MB.

The TOC/TOC_0 of MB is shown in Fig. 5(b). When these data were compared after a reaction time of 120 min, we found that the TOC/TOC_0 ratio in the PC or PEC system was approximately 0.73, which is higher than that in the MFC-PEC or MFC-EC system and indicates a lower degree of mineralization. In the MFC-PEC system, much fewer pollutants remained; the remaining TOC/TOC_0 was 0.17 after 120 min, which indicates that MB can be degraded and mineralized more thoroughly and stably in our new MFC-PEC system.

Similarly, tests were performed to examine the destruction of tetracycline. The degradation of COD in the tetracycline solution, which also signifies the degree of mineralization, is shown in Fig. 6. After 120 min, 70% of the COD was destroyed in the MFC-PEC system for an initial tetracycline concentration of 100 $mg \cdot L^{-1}$, whereas

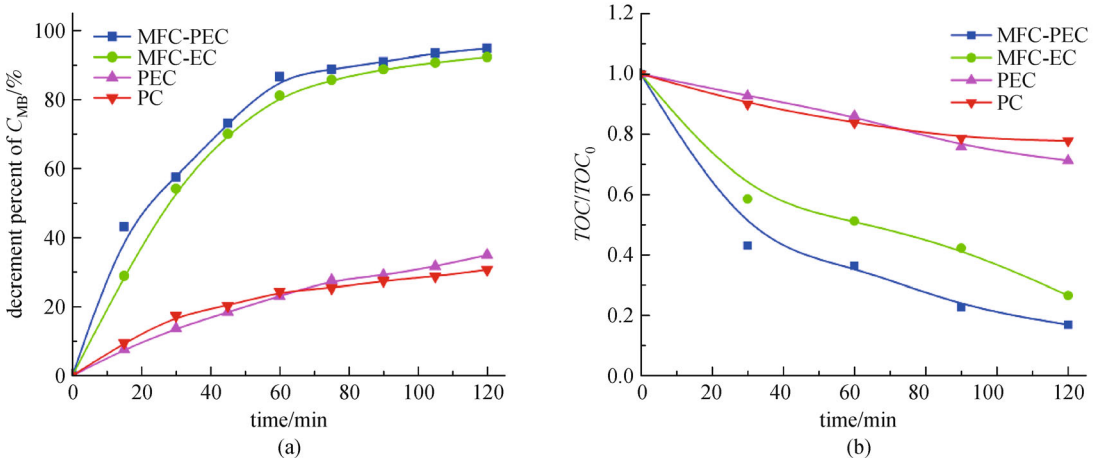

Fig. 5 Destruction of methylene blue (MB) under different conditions ((a) shows the decrement percent of concentration in the MB solution; (b) shows the change in TOC/TOC_0 in the MB solution)

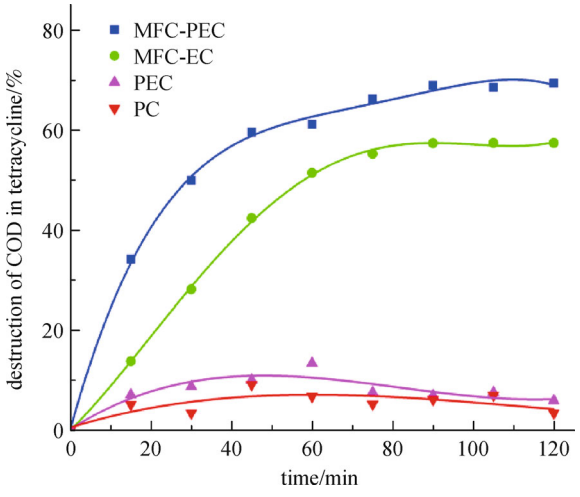

Fig. 6 Destruction of tetracycline under different conditions

approximately 57% of the COD was destroyed in the PEC-EC system. However, the PC and PEC systems could only degrade approximately 10% COD of the tetracycline. Figure 6 demonstrates that our new PEC-MFC system efficiently destroys tetracycline.

3.3 Analysis of radical species using ESR

Figure 7 displays the ESR spectrum of the trapped radicals during the MB test in our new system with and without light. The ESR spectroscopy is the most powerful instrument to investigate radical species. When well-resolved spectra can be observed, the spectra provide information about the structures, properties and concentration of the radicals and the initiating and propagating (oligomeric and polymeric) radicals [33].

During the test, DMPO, which is a type of high-efficiency ROS spin trap, was used because many free radicals are unstable and can form spin adducts, such as DMPO-OH and DMPO-OOH. The DMPO-OH spectrum has 4 spectral lines, whose strength ratio is 1 : 2 : 2 :1, which is a significant symbol when we identify ·OH. Thus, the signals in Fig. 7(a) were from the generated ·OH radicals. The signals of $\cdot O_2^-$ were also distinctively mixed in the spectra (Fig. 7(b)). These findings indicate that ·OH plays a major role in the degradation/oxidation process. Without light irradiation, the formed $\cdot O_2^-$ radicals can also contribute to the degradation of organic pollutants, although photolysis can also cause the pollutants to degrade.

3.4 Degradation mechanisms

For both the MFC-PEC and MFC-EC systems, electrons are generated by the metabolism of electricigens and passed to the cathode through the external circuit. An electron on the catalyst surface can activate O_2 to form $\cdot O_2^-$, which may further form H_2O_2 then ·OH, which is a powerful radical oxidant, according to Fig. 7.

According to the literature, TiO_2 has a conduction band of −0.2 V to −0.65 V and a valence band of 2.6–3.0 eV [34], which can provide electrons to reduce O_2 to $\cdot O_2^-$ (E^0 = 0.284 V *vs.* SHE) [33] and reduce Fe^{3+} and Fe^{2+} ($Fe^{3+} + e^- \rightarrow Fe^{2+}$, E^0 = 0.771 eV; $Fe^{2+} + 2e^- \rightarrow Fe^0$, E^0 = −0.44 eV) [35]. In the MFC-PEC and MFC-EC systems, a portion of the electrons from the bio-anode are transferred to the cathode though the external circuit. While irradiated by visible light, Fe^0/TiO_2 can also generate electrons. A portion of the electrons from the bio-anode and Fe^0/TiO_2 react with O_2 and form $\cdot O_2^-$. When electrons are excited on the Fe^0/TiO_2 surface, holes are simultaneously created, which can react with H_2O in the solution and form H_2O_2 then ·OH. As previously mentioned, if Fe^0 is oxidized to Fe^{2+} or Fe^{3+}, part of the electrons from the bio-anode and Fe^0/TiO_2 can reduce it back to Fe^0 again [27]. Hence, Fe^0 is

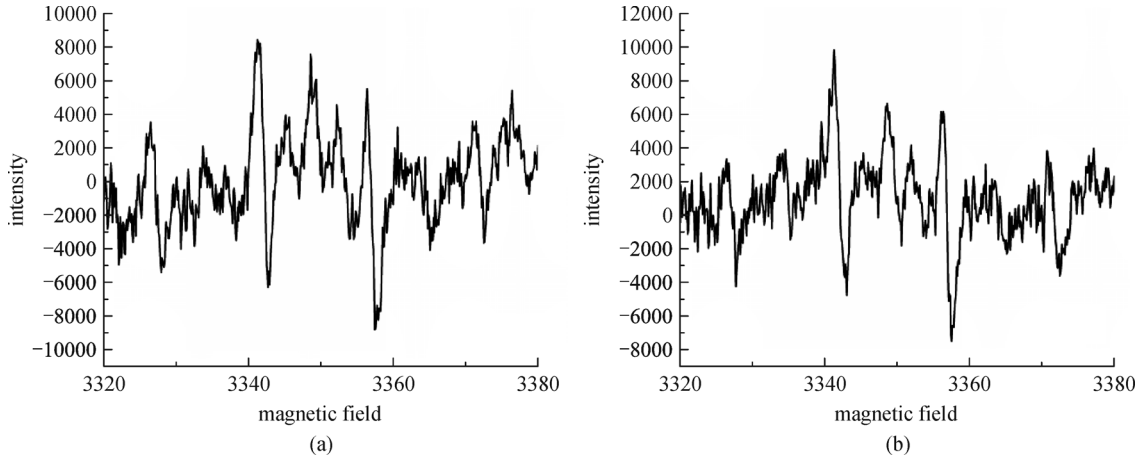

Fig. 7 ESR spectrum of the experiment when MB was removed from the system with light (a) and without light (b)

recycled. The degradation pathway can be described as follows [36]:

$$\text{Electricigens} \rightarrow \text{Electricigens} + e_E^- \quad (2)$$

$$Fe^0/TiO_2 + h\nu \rightarrow Fe^0/TiO_2(e_{CB}^- + h_{VB}^+) \quad (3)$$

$$e_{CB}^- \text{ or } e_E^- + O_2 \rightarrow \cdot O_2^- \quad (4)$$

$$h_{VB}^+ + H_2O \rightarrow \cdot OH + H^+ \quad (5)$$

$$\cdot O_2^- + 2H^+ + e_{CB}^- \text{ or } e_E^- \rightarrow H_2O_2 \quad (6)$$

$$H_2O_2 + h\nu \rightarrow \cdot OH + OH^- \quad (7)$$

$$Fe^0 \rightarrow Fe^{2+} + e_{Fe}^- \quad (8)$$

$$Fe^{2+} \rightarrow Fe^{3+} + e_{Fe}^- \quad (9)$$

$$MB + h_{VB}^+ \rightarrow [\text{Oxidized}] \text{ products} \quad (10)$$

$$MB + e_{CB}^- \text{ or } e_E^- \text{ or } e_{Fe}^- \rightarrow [\text{Reduced}] \text{ products} \quad (11)$$

$$MB + \cdot OH \rightarrow \text{Mineralized end products} \quad (12)$$

$$Fe^{3+} \text{or } Fe^{2+} + e_{CB}^- \text{ or } e_E^- \rightarrow Fe^0 \quad (13)$$

3.5 Cell voltage and power density

In Fig. 6, the cell voltages and power densities are shown: (1) the cathode was only SSM (under visible light); (2) the cathode was SSM with Fe^0/TiO_2 (MFC-PEC); and (3) the cathode was SSM with Fe^0/TiO_2 (MFC-EC). In addition, 20 $mg \cdot L^{-1}$ MB was used in all experiments.

The MFC-PEC system achieved a maximum cell voltage of 0.098 V. When the cathode was only SSM, the stable voltage only reached 0.064 V. All of the cell voltages decreased at first, slowly increased, and finally became constant with increasing reaction time. The power density similarly changed with the cell voltage. The maximum power density that was generated by the MFC-PEC system was 13.72 $mW \cdot m^{-2}$.

Figures 4 and 8 show that the cell voltage and power density increased when light is irradiated onto the cathode chamber with increased pollutant degradation. Although the decreases in MB concentration in MFC-PEC and MFC-EC were notably close (Fig. 5(a)), the MFC-PEC system generated a higher cell voltage than MFC-EC. This system may be operated under irradiation (MFC-PEC) and can achieve higher efficiency in water treatment and generate more electricity. Because the catalyst can catalyze the reactions and generate electricity without light, it can also operate in the dark (MFC-EC), although the treatment efficiency is slightly lower, and less electricity is generated.

3.6 Electrical energy efficiency

As previously mentioned, we calculated E_{Eo} for the different systems according to Fig. 4(a). E_{Eo} for the MFC-PEC system with 50 Watt visible light was approximately 0.675 $kWh \cdot m^{-3} \cdot order^{-1}$, whereas that for the MFC-EC system was zero. For comparison, E_{Eo} for the UV/TiO_2 system was approximately 0.045 $kWh \cdot m^{-3} \cdot order^{-1}$. These values show that our new MFC-EC system performs better than PEC and PC because it does not require an external light energy input. We also calculated the EC ($kWh \cdot m^{-3}$) per volume of treated working solution of our cell according to the literature [37], and the result was negligible (10^{-5} $kWh \cdot m^{-3}$).

4 Conclusions

A new system, MFC-PEC or MFC-EC, which couples PEC or EC with a MFC, has been constructed. It can

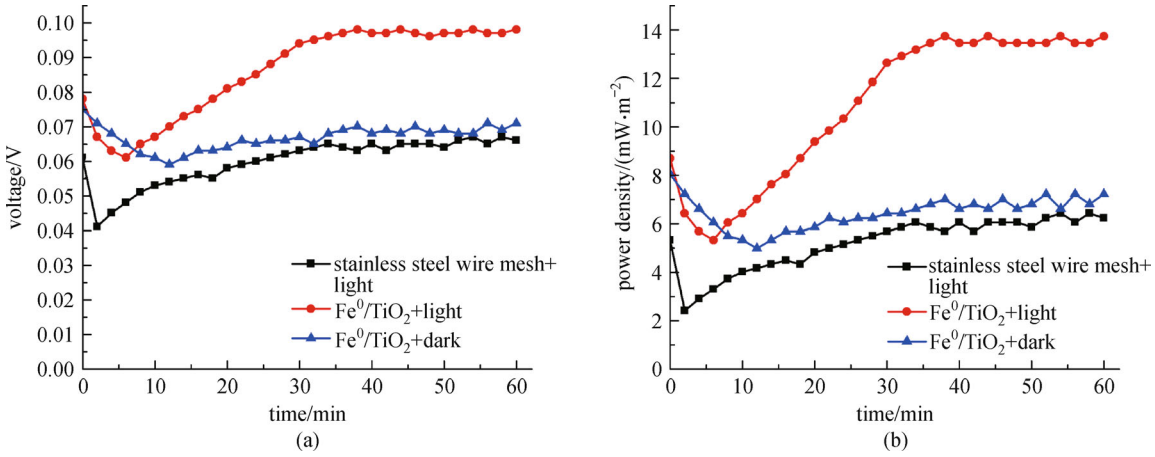

Fig. 8 Reactor cell voltage (a) and power density (b) under different conditions

degrade both methylene blue and tetracycline in the cathode chamber. This system degrades typical pollutants more efficiently and effectively than pure PC or PEC systems (using Fe^0/TiO_2 as the anode catalyst and Pt as the cathode catalyst) and at a lower cost. The bio-electricity assists the oxygen reduction over Fe^0/TiO_2, which forms ROS and facilitates the pollutant degradation. This system is more sustainable and carbon-neutral for potential applications. The MFC-PEC has the best performance in degrading pollutants and generating electricity, and it can operate both with and without light. With light, the MFC-PEC results in more efficient water treatment and generates more electricity. In the dark, the MFC-EC also works well. Further research is necessary to study the degradation pathways, although that issue does not diminish the prospects for practical application.

Acknowledgements This study was supported by the National Natural Science Foundation of China (Grant No. 21177018) and the Program of Introducing Talents of Discipline to Universities (B13012). The authors also appreciate the support from the Brook Byers Institute for Sustainable Systems, Hightower Chair and the Georgia Research Alliance at Georgia Institute of Technology.

References

1. Liu Y B, Li J H, Zhou B X, Li X J, Chen H C, Chen Q P, Wang Z S, Li L, Wang J L, Cai W M. Efficient electricity production and simultaneously wastewater treatment via a high-performance photocatalytic fuel cell. Water Research, 2011, 45(13): 3991–3998
2. Lin L, Wang H Y, Luo H M, Xu P. Enhanced photocatalysis using side-glowing optical fibers coated with Fe-doped TiO_2 nanocomposite thin films. Journal of Photochemistry and Photobiology A Chemistry, 2015, 307–308: 88–98
3. Chen Q P, Bai J, Li J H, Huang K, Li X J, Zhou B X, Cai W M. Aerated visible-light responsive photocatalytic fuel cell for wastewater treatment with producing sustainable electricity in neutral solution. Chemical Engineering Journal, 2014, 252: 89–94
4. Lai B, Wang P, Li H R, Du Z W, Wang L J, Bi S C. Calcined polyaniline-iron composite as a high efficient cathodic catalyst in microbial fuel cells. Bioresource Technology, 2013, 131: 321–324
5. Li J Y, Li J H, Chen Q P, Bai J, Zhou B X. Converting hazardous organics into clean energy using a solar responsive dual photoelectrode photocatalytic fuel cell. Journal of Hazardous Materials, 2013, 262: 304–310
6. Jadhav D A, Ghadge A N, Ghangrekar M M. Enhancing the power generation in microbial fuel cells with effective utilization of goethite recovered from mining mud as anodic catalyst. Bioresource Technology, 2015, 191: 110–116
7. Lee K Y, Ryu W S, Cho S I, Lim K H. Comparative study on power generation of dual-cathode microbial fuel cell according to polarization methods. Water Research, 2015, 84: 43–48
8. Wang A J, Cheng H Y, Ren N Q, Cui D, Lin N, Wu W M. Sediment microbial fuel cell with floating biocathode for organic removal and energy recovery. Frontiers of Environmental Science and Engineering, 2012, 6(4): 569–574
9. Liang P, Wei J C, Li M, Huang X. Scaling up a novel denitrifying microbial fuel cell with an oxic-anoxic two stage biocathode. Frontiers of Environmental Science and Engineering, 2013, 7(6): 913–919
10. Liu W F, Cheng S A, Sun D, Huang B, Chen J, Cen K F. Inhibition of microbial growth on air cathodes of single chamber microbial fuel cells by incorporating enrofloxacin into the catalyst layer. Biosensors & Bioelectronics, 2015, 72: 44–50
11. Liao Z H, Sun J Z, Sun D Z, Si R W, Yong Y C. Enhancement of power production with tartaric acid doped polyaniline nanowire network modified anode in microbial fuel cells. Bioresource Technology, 2015, 192: 831–834
12. Xiao Y, Zheng Y, Wu S, Yang Z H, Zhao F. Nitrogen recovery from wastewater using microbial fuel cells. Frontiers of Environmental Science and Engineering, 2016, 10(1): 185–191
13. Wang Z J, Zhang B G, Alistair G L B, Feng C Q, Ni J R. Utilization of single-chamber microbial fuel cells as renewable power sources for electrochemical degradation of nitrogen-containing organic compounds. Chemical Engineering Journal, 2015, 280: 99–105
14. Tang W W, Chen X Y, Xia J, Gong J M, Zeng X P. Preparation of an

Fe-doped visible-light-response TiO_2 film electrodeand its photo-electrocatalytic activity. Materials Science and Engineering B, 2014, 187: 39–45

15. Ding X, Ai Z H, Zhang L Z. A dual-cell wastewater treatment system with combining anodic visible light driven photoelectro-catalytic oxidation and cathodic electro-Fenton oxidation. Separation and Purification Technology, 2014, 125: 103–110
16. Li J, Lv S, Liu Y, Bai J, Zhou B, Hu X. Photoeletrocatalytic activity of an n-ZnO/p-Cu_2O/n-TNA ternary heterojunction electrode for tetracycline degradation. Journal of Hazardous Materials, 2013, 262: 482–488
17. Liu Y B, Li H, Zhou B X, Lv S B, Li X J, Chen H C, Chen Q P, Cai W M. Photoelectrocatalytic degradation of refractory organic compounds enhanced by a photocatalytic fuel cell. Applied Catalysis B: Environmental, 2012, 111–112: 485–491
18. Xu S C, Pan S S, Xu Y, Luo Y Y, Zhang Y X, Li G H. Efficient removal of Cr(VI) from wastewater under sunlight by Fe(II)-doped TiO_2 spherical shell. Journal of Hazardous Materials, 2015, 283: 7–13
19. Chen C, Long M C, Zeng H, Cai W M, Zhou B X, Zhang J Y, Wu Y, Ding D W, Wu D Y. Preparation, characterization and visible-light activity of carbon modified TiO_2 with two kinds of carbonaceous species. Journal of Molecular Catalysis A Chemical, 2009, 314(1–2): 35–41
20. Yao Y, Li K, Chen S, Ji J P, Wang Y L, Wang H W. Decolorization of Rhodamine B in a thin-film photoelectrocatalytic (PEC) reactor with slant-placed TiO_2 nanotubes electrode. Chemical Engineering Journal, 2012, 187: 29–35
21. Hsieh W P, Pan J R, Huang C, Su Y C, Juang Y J. Enhance the photocatalytic activity for the degradation of organic contaminants in water by incorporating TiO_2 with zero-valent iron. Science of the Total Environment, 2010, 408(3): 672–679
22. Rodriguez S, Vasquez L, Costa D, Romero A, Santos A. Oxidation of Orange G by persulfate activated by Fe(II), Fe(III) and zero valent iron (ZVI). Chemosphere, 2014, 101: 86–92
23. Wang Z Q, Wen B, Hao Q Q, Liu L M, Zhou C, Mao X, Lang X, Yin W J, Dai D, Selloni A, Yang X. Localized excitation of Ti^{3+} ions in the photoabsorption and photocatalytic activity of reduced rutile TiO_2. Journal of the American Chemical Society, 2015, 137(28): 9146–9152
24. Xu Y L, Jia J P, Zhong D J, Wang Y L. Degradation of dye wastewater in a thin-film photoelectrocatalytic (PEC) reactor with slant-placed TiO_2/Ti anode. Chemical Engineering Journal, 2009, 150(2–3): 302–307
25. Yang J, Cao M, Guo R, Jia J P. Permeable reactive barrier of surface hydrophobic granular activated carbon coupled with elemental iron for the removal of 2,4-dichlorophenol in water. Journal of Hazardous Materials, 2010, 184(1–3): 782–787
26. Kim J H, Park I S, Park J Y. Electricity generation and recovery of iron hydroxides using a single chamber fuel cell with iron anode and air-cathode for electrocoagulation. Applied Energy, 2015, 160: 18–27
27. Liu L F, Chen F, Yang F L, Che Y S, Crittenden J. Photocatalytic degradation of 2,4-dichlorophenol using nanoscale Fe/TiO_2. Chemical Engineering Journal, 2012, 181–182: 189–195
28. Daneshvar N, Aber S, Seyed Dorraji M S, Khataee A R, Rasoulifard M H. Photocatalytic degradation of the insecticide diazinon in the presence of prepared nanocrystalline ZnO powders under irradiation of UV-C light. Separation and Purification Technology, 2007, 58(1): 91–98
29. Muruganandham M, Selvam K, Swaminathan M. A comparative study of quantum yield and electrical energy per order (E_{Eo}) for advanced oxidative decolourisation of reactive azo dyes by UV light. Journal of Hazardous Materials, 2007, 144(1–2): 316–322
30. Daneshvar N, Aleboyeh A, Khataee A R. The evaluation of electrical energy per order (E_{Eo}) for photooxidative decolorization of four textile dye solutions by the kinetic model. Chemosphere, 2005, 59(6): 761–767
31. Behnajady M A, Vahid B, Modirshahla N, Shokri M. Evaluation of electrical energy per order (E_{Eo}) with kinetic modeling on the removal of Malachite Green by US/UV/H_2O_2 process. Desalination, 2009, 249(1): 99–103
32. He C, Yu Y, Hu X F, Larbot A. Influence of silver doping on the photocatalytic activity of titania films. Applied Surface Science, 2002, 200(1–4): 239–247
33. Atsushi K.A combination of Electron Spin Resonance spectroscopy/atom transfer radical polymerization (ESR/ATRP) techniques for fundamental investigation of radical polymerizations of (meth) acrylates. Polymer, 2015, 72: 253–263
34. Fujishima A, Zhang X, Tryk D A. TiO_2 photocatalysis and related surface phenomena. Surface Science Reports, 2008, 63(12): 515–582
35. Huang C, Hsieh W P, Pan J R, Chang S M. Characteristic of an innovative TiO_2/Fe^0 composite for treatment of azo dye. Separation and Purification Technology, 2007, 58(1): 152–158
36. Jayanthi Kalaivani G, Suja S K. TiO_2 (rutile) embedded inulin—A versatile bio-nanocomposite for photocatalytic degradation of methylene blue. Carbohydrate Polymers, 2016, 143: 51–60
37. Shestakova M, Graves J, Sitarz M, Sillanpää M. Optimization of Ti/Ta_2O_5–SnO_2 electrodes and reaction parameters for electrocatalytic oxidation of methylene blue. Journal of Applied Electrochemistry, 2016, 46(3): 349–358